

# The Impact of Travelling On The COVID-19 Infection Cases in Germany

Moritz Schäfer (✉ [moritzschaefer@uni-koblenz.de](mailto:moritzschaefer@uni-koblenz.de))

University of Koblenz-Landau

Karunia Putra Wijaya

University of Koblenz-Landau

Robert Rockenfeller

University of Koblenz-Landau

Thomas Götz

University of Koblenz-Landau

---

## Research Article

**Keywords:** COVID-19, Infection, SEIRD

**Posted Date:** July 6th, 2021

**DOI:** <https://doi.org/10.21203/rs.3.rs-538681/v2>

**License:** © ⓘ This work is licensed under a Creative Commons Attribution 4.0 International License.

[Read Full License](#)

---

# The Impact of Travelling on the COVID–19 Infection Cases in Germany

Moritz Schäfer<sup>1,\*</sup>, Karunia Putra Wijaya<sup>1</sup>, Robert Rockenfeller<sup>1</sup>, and Thomas Götz<sup>1</sup>

\*Corresponding author. Mail address: [moritzschaefer@uni-koblenz.de](mailto:moritzschaefer@uni-koblenz.de)

<sup>1</sup>Mathematical Institute, University of Koblenz–Landau, 56070 Koblenz, Germany

## ABSTRACT

### Background

COVID–19 continues to disrupt social lives and the economy of many countries and challenges their healthcare capacities. In Germany, the number of cases increased exponentially in early March 2020. As a political reaction, social restrictions were imposed by closing e.g. schools, shops, cafés and restaurants, as well as borders for travellers. This reaped success as the infection rate descended significantly in early April. In mid July, however, the numbers started to rise again. Of particular reasons was that from 15 June onwards, the travel ban has widely been cancelled or at least loosened.

### Methods

Here, we present an extended susceptible–exposed–infected–recovered–deceased (SEIRD) model to describe the disease dynamics in Germany, taking into account German travellers which returned infected from abroad. Epidemiological parameters like transmission rate, lethality or detection rate of infected individuals, as well as a rate measuring the impact of these travellers, were estimated by fitting the model output to available data. Parameter estimation was performed via Bayesian inference with the aid of the Monte–Carlo–based Metropolis algorithm.

### Results

We found that travellers had a strong impact on the overall infection cases. Until the end of August, roughly 50,000 cases directly or indirectly related to travellers were estimated. These obviously caused even higher infection cases later on, which among other causes lead to a second wave of infection cases in late 2020.

### Conclusions

We conclude that travel restrictions are an important tool for controlling infection cases during pandemics which can still have an impact on the upcoming summer in case the currently high vaccination rates can not prevent further infection waves.

## Introduction

The COVID-19 disease in Germany started with a first infection case on 26 January 2020 in Bavaria<sup>1</sup>. In March, the number of cases grew rapidly (with a maximum of 6933 cases on 27 March), and various social restrictions were imposed as an active intervention of the disease<sup>2,3</sup>. On June 10, only 16 new infections with the virus were detected<sup>2</sup>. In mid June, travel restrictions were relaxed for travels within Europe<sup>4</sup>. However, the pandemic continues to spread worldwide and by the end of August, new maxima for the daily cases worldwide set another record<sup>5</sup>. After or towards the end of the summer holidays in the first German states in mid to end of August, a second rise of infection cases could also be seen, with around or more than 1,000 new infections per day<sup>2</sup>. Fig. 1 shows the temporal evolution of COVID-19 cases in Germany from 26 January until 31 August.

According to the Robert Koch Institute (RKI) in Germany, many of the cases from June onwards were directly related to German travellers returning home<sup>6</sup>. The impact of travellers to the disease epidemics is a part of ongoing research. Berestycki et al. investigate diffusion effects, especially along major roads<sup>7</sup>. Siegenfeld et al. studied the impact of region-to-region travelling<sup>8</sup>. Chinazzi et al. regarded the impact of travel restrictions in China on the worldwide disease spread<sup>9</sup>. Our study makes use of a susceptible–exposed–infected–recovered–deceased (SEIRD) model introduced in the previous work of Heidrich et al.<sup>10</sup> to model the confirmed cases for several countries worldwide, adding relevant numbers of German travellers. We

estimate model parameters by using the available data from the Johns-Hopkins University (JHU)<sup>2</sup>. The estimation itself is based on a least-squares fit between the model output and the reported data. Here, both the reported infections and fatalities are taken into account. As a next step, we update the SEIRD model for Germany, including travellers, and estimate not only the "classic" parameters as of<sup>10</sup> but also the impact of the infected travellers to the overall epidemics.

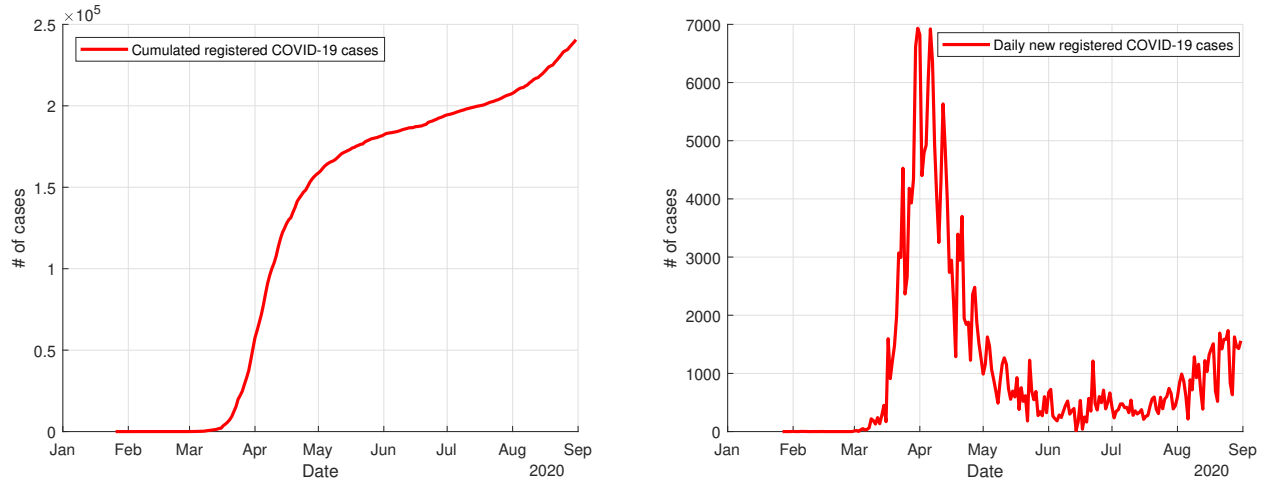


**Figure 1.** Number of COVID-19 confirmed cases (left) and daily cases (right) in Germany from January 26 until August 31, 2020 according to Johns Hopkins University.

## Model

In the previous work we investigated the dynamics of COVID-19 disease until early May 2020<sup>10</sup>; this study builds up on this approach. Again we use a variation of the SIR-model introduced by McKendrick<sup>11</sup>; see also Martcheva<sup>12</sup> for an overview of mathematical models in epidemiology. It builds up on delayed differential equation (DDE) system to describe the behaviour of the disease in Germany in summer 2020. The entire population  $N$  is subdivided into five compartments: susceptible  $S$ , exposed  $E$ , infected  $I$ , recovered  $R$ , and deceased  $D$ . The virus is transmitted from infected persons to susceptible persons at a piecewise constant rate  $\beta$ . After an incubation duration  $\kappa^{-1}$  exposed individuals become infective. Loss of infectivity is gained after an average duration  $\gamma^{-1}$ ; the death rate  $\mu$  describes the fraction of persons dying from the disease. A time lag  $\tau$  between the infected and the deceased state accounts for the fact that the number of people dying from the disease is attained from the infected number  $\tau$  days earlier. Here, we also introduce an additional compartment: travellers  $E_t$  which have been exposed to the disease abroad. Values for the fixed model parameters in Germany are given in Tab. 1.

Parameter	Value	Reference
$N$	83,019,213	<sup>13</sup>
$\kappa$	$(3 \text{ d})^{-1}$	<sup>14</sup>
$\gamma$	$(10 \text{ d})^{-1}$	<sup>14</sup>

**Table 1.** Used parameter values.

These assumptions lead us to the following five-dimensional ODE system:

$$S' = -\frac{\beta}{N}SI - E_T(t) \quad S(t_0) = S_0 = N - E_0 - I_0 - R_0 - D_0 > 0 \quad (1a)$$

$$E' = \frac{\beta}{N}SI + E_T(t) - \kappa E \quad E(t_0) = E_0 \geq 0 \quad (1b)$$

$$I' = \kappa E - \gamma((1 - \mu)I + \mu I(t - \tau)) \quad I(t_0 - \tau \leq t \leq t_0) = \varphi(t) > 0 \quad (1c)$$

$$R' = (1 - \mu)\gamma I \quad R(t_0) = R_0 \geq 0 \quad (1d)$$

$$D' = \mu\gamma I(t - \tau) \quad D(t_0) = D_0 \geq 0 \quad (1e)$$

The function  $\varphi : [t_0 - \tau, t_0] \rightarrow \mathbb{R}_+$  denotes the initial history of the infected required for the well-posedness of the above DDE. Also, the number of travellers which have been exposed to the disease is defined as

$$E_T(t) = \alpha(t) \sum_j \frac{\beta_j(t)}{N_j} \cdot T_{\text{Germany} \leftrightarrow j}(t) \cdot I_j. \quad (2)$$

The values  $I_j$  and  $N_j$  are defined by the number of infected people and respectively the resident population in country  $j \neq \text{Germany}$  at time  $t$ . The parameter  $T_{\text{Germany} \leftrightarrow j}(t)$  describes the number of travellers from Germany to country  $j$ . Due to monthly available travelling data,  $\alpha(t)$  quantifies the special risk of getting infected as a traveller, as this should obviously differ from the average inhabitant. If  $\alpha \equiv 1$ , the transmission rate for travellers is equal to the country's specific transmission rate  $\beta_j(t)$ . This rate is piecewise constant with switching returned from imposition or relaxation of certain measures. No inclusion of travellers due to bans or closed borders are identical to  $\alpha \equiv 0$ .

The parameters of  $\beta_j(t)$  as well as  $I_j$  and  $N_j$  are estimated by using the SEIRD model without a traveller compartment:

$$S'_j = -\frac{\beta_j(t)}{N_j} S_j I_j \quad S_j(t_0) = S_{j,0} = N_j - E_{j,0} - I_{j,0} - R_{j,0} - D_{j,0} > 0 \quad (3a)$$

$$E'_j = \frac{\beta_j(t)}{N_j} S_j I_j - \kappa E_j \quad E_j(t_0) = E_{j,0} \geq 0 \quad (3b)$$

$$I'_j = \kappa E_j - \gamma((1 - \mu_j)I_j + \mu_j I_j(t - \tau_j)) \quad I_j(t \leq t_0) = \varphi_j(t) > 0 \quad (3c)$$

$$R'_j = (1 - \mu_j) \gamma I_j \quad R_j(t_0) = R_{j,0} \geq 0 \quad (3d)$$

$$D'_j = \mu_j \gamma I_j(t - \tau_j) \quad D_j(t_0) = D_{j,0} \geq 0 \quad (3e)$$

The values for  $\kappa$  and  $\gamma$  are assumed to be independent of country  $j$ . The reasons of the higher infection rate are not relevant for the infection process in the main model. Instead of a raising number of travellers, we therefore impose two different transmission rates  $\beta_0$  and  $\beta_1$  for the various countries:

$$\beta_j(t) := \begin{cases} \beta_{j,0}, & t \leq 19 \text{ July} \\ \beta_{j,1}, & 20 \text{ July} \leq t \end{cases} \quad (4)$$

The starting point  $t_0$  is chosen as 1 June because of travel restrictions being relaxed as of 15 June<sup>15</sup>, so that the transmission rate  $\beta$  is not correlated to the travel impact rate  $\alpha$  during the optimization process. The end date is fixed to 31 August because of the available data and new restrictions in other countries from September onwards, e.g. a travel warning for Spain<sup>4</sup>, which will affect the transmission parameters.

The parameters  $N_j$  reflect the current total populations in all regarded countries which are the destination or origin of travellers from and to Germany; the population data is taken from<sup>13</sup>. We only include European countries with available traveller statistics and countries outside of Europe with a total sum of more than 5,000 travellers in the travelling statistics. For the close European countries, the number of travellers is estimated by the travel statistics of 2019 for German travellers<sup>16</sup> and hospitality statistics in Germany for foreign travellers<sup>17</sup>. The number of travellers from and to farther and non-European countries is gained from analysis of the flight passengers from the respective country<sup>18</sup>. For larger countries like USA, Russia, China and Japan the estimations were problematic (mainly due to a high number of non-direct flight routes), so we assumed them to be the same as the number of travellers from the respective country to Germany, for which data is available. The populations and amount of travellers per month of this total of 55 countries is presented in Tab. 2.

By using this table, we can compute the daily value for  $T_{\text{Germany} \leftrightarrow j}$  by the number of travellers divided by the days in the respective month. E.g., for June, only the 16 days from 15 June to 30 June are considered. Average time of spending time here is 12 days so e.g. for July,  $T_{\text{Germany} \leftrightarrow \text{Spain}} = 331,894 \cdot \frac{12}{31\text{d}} \approx 128,475 \text{ d}^{-1}$ . The uncertainty in the value of 12 days for the average travel length is mitigated by the estimation of  $\alpha$ , as these two values are directly multiplied and thus only the product of those two values is important.

In a first model,  $\alpha(t)$  is assumed to be constant over time as soon as the travel ban is loosened:

$$\alpha(t) := \begin{cases} 0 & t \leq 14 \text{ June} \\ \alpha & 15 \text{ June} \leq t \leq 31 \text{ August} \end{cases} \quad (5)$$

In the second model, we define a piecewise constant  $\alpha(t)$  as follows:

$$\alpha(t) := \begin{cases} 0 & t \leq 14 \text{ June} \\ \alpha_0 & 15 \text{ June} \leq t \leq 30 \text{ June} \\ \alpha_1 & 1 \text{ July} \leq t \leq 31 \text{ July} \\ \alpha_2 & 1 \text{ August} \leq t \leq 31 \text{ August} \end{cases} \quad (6)$$

This way, we are able to identify temporal differences in the travelling compartment, e.g. caused by a different social behaviour or loosened restrictions.

## Parameter estimation

### Likelihood function

The unknown parameter set  $u$  will be estimated using a least squares fit of the model output with respect to the given data. Let  $Y = (Y_i)$  and  $Z = (Z_i)$  denote the accumulated confirmed cases and deaths related to COVID-19 in Germany. The subscript  $i$  serves to point out the measurement at time point  $t_i$ . Also, let  $Y^j = (Y_i^j)$  and  $Z^j = (Z_i^j)$  denote the infection and death cases in the destination country as reported by the JHU<sup>2</sup>. The reported cases  $Y$  and  $Y^j$  consist of the currently infected cases, the recovered, and deceased cases. Not all infections are by nature detected, from which case we introduce detection rates  $\delta$  for Germany and  $\delta_j$  for the destination country, respectively. For the persons which are currently infected or have recovered, we assume that only this proportion  $\delta$  or  $\delta_j$  is tested and detected and hence appears in the statistics; however, we assume no undetected deceased cases. We assume that the proportion of detected cases versus real infections is constant over the whole time interval, so that no temporal change of the detection rate is needed in our model. Hence we compare the data  $Y$  to  $\delta \cdot (I + R) + D := C$  and  $Y^j$  to  $\delta_j \cdot (I_j + R_j) + D_j := C_j$  from the model output. The initial value of the infected cases at the starting date 1 June and 15 June is later on subject of the estimation procedure. Therefore, we use the infected data as the real data divided by the detection rate, for Germany and destination countries, respectively:

$$\varphi(t) := \frac{\text{interp}\{(Y_i)\}(t)}{\delta} \quad t_0 - \tau \leq t \leq t_0, \quad (7)$$

$$\varphi_j(t) := \frac{\text{interp}\{(Y_i^j)\}(t)}{\delta_j} \quad t_0 - \tau_j \leq t \leq t_0. \quad (8)$$

At time  $t_i$ , our model validation is subject to measurement error, which is assumed to be of degenerate multivariate Gaussian distribution with mean  $(Y_i, Z_i)$  or  $(Y_i^j, Z_i^j)$  and covariance matrix  $\Sigma$  or  $\Sigma^j$ , where one covariate corresponds to the measurement error from confirmed cases and the other to the deceased cases. The time invariance of the covariance matrix was opted only for the sake of simplicity. Further simplification may assert prior assumption that the covariance terms in the measurement error are zero, meaning that each error is an independent process. This leads us to  $\Sigma = \text{diag}(\sigma_Y, \sigma_Z)$  or  $\Sigma^j = \text{diag}(\sigma_Y^j, \sigma_Z^j)$ . Our likelihood function to be maximized for only time point  $t_i$  reads as

$$L_i(u) := \frac{1}{2\pi\sigma_Y\sigma_Z} \exp\left(-\frac{(\delta[I(t_i) + R(t_i)] + D(t_i) - Y_i)^2}{\sigma_Y^2} - \frac{(D(t_i) - Z_i)^2}{\sigma_Z^2}\right). \quad (9)$$

Assuming iid processes for all measurements at all time points, Kalbfleisch in<sup>19</sup> pointed out a constant  $K$  that serves to simplify the joint likelihood function

$$L(u) := K \prod_i L_i(u) = \frac{K}{(2\pi)^N} \cdot \frac{1}{\sigma_Y^N \sigma_Z^N} \exp\left(-\sum_i \frac{(\delta[I(t_i) + R(t_i)] + D(t_i) - Y_i)^2}{\sigma_Y^2} + \frac{(D(t_i) - Z_i)^2}{\sigma_Z^2}\right). \quad (10)$$

Typically the constant is specified as  $K = (2\pi)^N$ . Our study designates the standard deviations as to approximate the means of confirmed and deceased cases,  $\sigma_Y := \|Y\|/N$  and  $\sigma_Z := \|Z\|/N$ . Hence, the likelihood and log-likelihood function read as

$$L(u) = \frac{N^{2N}}{\|Y\|^N \|Z\|^N} \exp\left(-\sum_i \frac{(\delta[I(t_i) + R(t_i)] + D(t_i) - Y_i)^2}{\|Y\|^2/N^2} + \frac{(D(t_i) - Z_i)^2}{\|Z\|^2/N^2}\right), \quad (11)$$

$$\log L(u) = \log\left(\frac{N^{2N}}{\|Y\|^N \|Z\|^N}\right) - \sum_i \frac{(\delta[I(t_i) + R(t_i)] + D(t_i) - Y_i)^2}{\|Y\|^2/N^2} + \frac{(D(t_i) - Z_i)^2}{\|Z\|^2/N^2}. \quad (12)$$

Country	Population	Travellers			Transmission	
		June	July	August	$\beta_{j,1}$	$\beta_{j,2}$
Decimal Power / Unit	$10^6$	1	1	1	$10^{-1}d^{-1}$	$10^{-1}d^{-1}$
Albania	2.88	945	3,366	9,505	1.20	1.19
Austria	8.90	312,364	636,414	782,818	1.35	1.36
Belarus	9.45	1,595	1,985	3,102	0.38	0.65
Belgium	11.51	36,210	155,295	92,495	1.17	1.60
Bosnia and Herzegovina	3.30	2,811	2,849	6,702	1.54	1.10
Brazil	211.05	6,715	4,366	3,778	1.22	1.12
Bulgaria	6.95	11,562	42,552	74,363	1.24	1.06
Canada	37.41	4,746	9,778	8,368	0.31	1.33
China	1,433.78	3,711	5,921	7,077	1.55	1.05
Croatia	4.06	66,029	84,952	150,790	0.31	1.10
Cyprus	0.89	360	7,191	14,049	0.42	1.89
Czech Republic	10.69	51,518	130,651	148,353	0.84	1.41
Denmark	5.81	48,986	395,924	571,649	0.77	1.70
Egypt	100.39	2,542	5,134	7,790	0.65	0.36
Estonia	1.33	1,006	3,380	5,967	0.23	2.00
Ethiopia	112.08	1,431	2,089	2,066	1.84	1.45
Finland	5.53	4,624	12,134	19,074	0.31	1.74
France	67.20	105,905	326,298	345,913	0.95	1.96
Greece	10.7	15,930	179,531	372,892	1.41	1.75
Hungary	9.77	30,154	53,080	71,577	0.36	1.71
Iceland	0.34	889	7,892	13,718	1.66	1.56
Ireland	4.97	4,892	8,965	9,065	0.43	2.20
India	1,366.42	5,168	8,676	14,046	1.39	1.25
Israel	88.52	2,455	2,693	797	1.65	1.23
Italy	60.29	126,855	272,324	415,581	0.21	1.75
Japan	126.86	1,457	2,340	3,292	1.78	1.29
Kosovo	1.72	586	7,341	18,626	1.59	1.10
Latvia	1.91	5,936	12,637	20,798	0.31	1.52
Lebanon	6.87	167	1,699	5,298	1.09	1.94
Lithuania	2.79	1,203	1,787	2,415	0.49	1.89
Luxembourg	0.63	4,562	4,466	2,946	2.54	0.51
Malta	0.51	261	9,338	16,974	1.16	1.95
Mexico	127.58	2,079	2,726	2,253	1.70	0.69
Montenegro	0.63	728	2,490	4,118	3.75	0.54
Moldova	4.04	972	1,728	3,815	0.85	1.30
Netherlands	17.40	188,840	721,721	1,592,831	1.04	1.72
Northern Macedonia	2.08	0	3,486	9,875	0.89	1.02
Norway	5.37	8,326	42,589	64,125	0.74	1.70
Poland	27.94	95,372	171,127	268,559	0.52	1.51
Portugal	10.29	17,659	63,369	111,867	0.51	0.81
Qatar	2.83	6,063	8,336	6,747	0.79	1.00
Romania	19.36	5,702	32,822	41,255	1.18	1.35
Russia	145.87	3,550	6,017	7,324	0.61	1.03
Serbia	8.77	5,164	5,577	9,672	1.62	0.61
Slovakia	5.46	19,372	31,161	56,401	1.16	1.54
Slovenia	2.07	3,759	5,361	5,987	1.44	1.14
Spain	47.32	22,209	331,894	436,624	1.19	1.86
Sweden	10.32	9,050	39,584	46,878	0.38	0.55
Switzerland	8.50	102,698	272,121	388,971	1.49	1.35
Tunisia	11.69	644	2,709	11,292	1.09	2.12
Turkey	83.43	36,986	144,350	343,972	0.77	1.14
United Kingdom	66.43	17,026	29,925	32,969	0.92	1.16
Ukraine	43.99	3,020	8,934	14,759	0.77	1.44
United States of America	329.06	24,123	42,409	41,613	0.81	1.62
United Arab Emirates	9.77	3,231	9,394	6,856	0.59	1.10

**Table 2.** Fixed parameter values for the population  $N_j$  as well as the (estimated) number of travellers per month  $T_{\text{Germany} \leftrightarrow j}$  in summer 2020 and the transmission parameters  $\beta_{j,1/2}$  by application of model (3).

We denote  $J(u)$  as the least square error of the estimation with respect to the data

$$J(u) = - \sum_i \frac{(\delta[I(t_i) + R(t_i)] + D(t_i) - Y_i)^2}{\|Y\|^2} + \frac{(D(t_i) - Z_i)^2}{\|Z\|^2}.$$

Then it holds

$$\log L(u) = N(2 \log N - \log \|Y\| - \log \|Z\| - NJ(u)). \quad (13)$$

Note that the same calculation can be done for the destination countries  $\log L_j(u)$ .

### Model specification

We researched variable choices for model specification, especially for the fitting of German data. The criterion is based on fit and complexity (information-type criterion). We opt for a minimal value of the Bayesian Information Criterion

$$\text{BIC} = -2 \log L + \log N \cdot |u| \quad (14)$$

according to<sup>20</sup>, whose first term represents maximal likelihood function and second term measures complexity represented by the observation size  $N$  and the number of parameters  $|u|$ . This BIC penalizes the number of parameters more than the Akaike Information Criterion (AIC)<sup>21</sup>, where the latter would have replaced the factor  $\log(N)$  by 2. As far as model specification is concerned, our aim will be to choose between three models toward cutting down BIC as well as amending the question if the role of travellers is significant.

- (A) without usage of an additional travel impact parameter, but with a time-dependent transmission rate  $\beta_2$  as of equations (3)
- (B) using a constant travel transmission parameter  $\alpha$  from 15 June onwards as of equations (1), (2) and (5)
- (C) using a piecewise linear travel transmission function  $\alpha(t)$  starting 15 June and jumps on 1 July and 1 August as of equations (1), (2) and (6)

### Bounds and initial values

The parameters to be estimated in models (1) and (3) are transmission rate, detection rate, lethality, time lag, travel impact rate and numbers of exposed on 1 June 2020 (Germany) respectively 15 June 2020 (all other countries), i.e.

$$u = (\beta, \delta, \mu, \tau, \alpha, E_0) \in \mathbb{R}^6, \quad (15)$$

$$u_j = (\beta_{j,0}, \beta_{j,1}, \delta_j, \mu_j, \tau_j, E_{0,j}) \in \mathbb{R}^6. \quad (16)$$

The optimal parameters  $u^*$  are determined by solving the following minimization problem:

$$\max_u L(u) \quad \text{subject to ODE (1)}, \quad (17)$$

$$\max_{u_j} L(u_j) \quad \text{subject to ODE (3)}. \quad (18)$$

Tab. 3 shows the planned simulations including constraints for the optimized parameters in  $u$ , which can also be used for  $u_j$  (with the starting value for the recovered as listed in<sup>2</sup>).

$\beta_{0/1}$	$\delta$	$\mu$	$\tau$	$\alpha_j$	$N_0$	$E_0$	$I_0$	$R_0$	$D_0$
$> 0.05$	$0.05 - 1$	$\leq 0.1$	$3 - 40$	$> 0$	82,846,340	$> 0$	$9,407/\delta$	$165,632/\delta$	8,555

**Table 3.** Simulations with the respective constraints of the fitted parameters. The starting values for  $R_0$  is only updated in the first two simulations by division with  $\delta$  in each iteration.

Previous investigations in<sup>22</sup> and<sup>10</sup> already give us orders of magnitude for the initial values of the optimization for  $\beta_j$  and  $\delta$ . The order of magnitude of the time interval between the onset of infectiousness and death is derived from the investigations in<sup>14</sup>. We allow a larger span in  $\tau$  and  $\tau_j$  than in<sup>10</sup> because the onset between infection and death is also dependent of the date on which the death case is transmitted, where significantly different values depending on the country can be seen. The starting values for  $I_0$  and  $R_0$  can be taken from the statistics. Depending on the value of the detection rate, the actual number is calculated by dividing the measured values for the infected and recovered cases by  $\delta$ . Regarding an estimate of the exposed

individuals  $E_0$  at time  $t_0$ , we use a derivation using the Basic Reproduction Number  $\mathcal{R}_0$ , which indicates how many new infections an infected individual causes on average during its illness in an otherwise susceptible population. In our model, the infected persons  $I_0$  are at different time stages during their infectiousness. As a mean value we assume the middle of this time interval. Thus, up to this point in time they could infect about  $I_0\mathcal{R}_0/2$  persons on average. Depending on the assumed Basic Reproduction Number, this results in different starting values for  $E_0$ . Here, we assume that the initial basic reproductive number is approximately  $\mathcal{R}_0 \approx 1$  because of the stagnation of cases on a low level at the beginning of June. Also, the initial number of infected is defined as  $I_0 = (Y_0 - R_0 - Z_0)/\delta$ .

param.	$\beta_{0/1}$	$\delta$	$\mu$	$\tau$	$\alpha_j$	$E_0$
init. val.	0.1	0.3	0.005	20	1	$I_0/2$

**Table 4.** Orders of magnitude of the initial values for adapting the model to the available data

### Metropolis algorithm

In our study, we use a Metropolis algorithm (cf.<sup>23–25</sup>) for estimation of parameters in models (1) and (3) according to the procedure described in<sup>26</sup> and<sup>10</sup>. Using the parameter set  $u_0$  as of Table 4 as starting conditions, we assign random draws  $u_{new}$  from a normally distributed (and thus symmetric) proposal function  $q$ , i.e.  $u_{new} \sim q(u_{new}|u_{i-1})$ , in every iteration  $i$ .

Using the previously defined  $J(u)$  as the target distribution, we calculate the approximative distribution by

$$\pi(u) = c \cdot \exp\left(-\frac{J(u)^2}{2\sigma^2}\right), \quad (19)$$

whereby  $c$  is an arbitrary real value. For the acceptance probability, it follows

$$p(u_{new}|u_{i-1}) = \min\left\{1, \frac{\pi(u_{new}) \cdot q(u_{i-1}|u_i)}{\pi(u_i) \cdot q(u_i|u_{i-1})}\right\} = \min\left\{1, \frac{\pi(u_{new})}{\pi(u_i)}\right\}. \quad (20)$$

In eq. (20) we can see that the value of  $c$  is redundant as it cancels out in the division. If the sample is accepted with the probability  $p$ , we set  $u_i = u_{new}$ ; with the probability  $1 - p$ , the sample is declined, meaning  $u = u_{i-1}$  according to<sup>26,27</sup>.

### Confidence intervals of the parameters

Considering that the observation size  $N$  and the number of parameters  $|u|$  hold the relation  $N \gg |u|$ , we adopt the idea of asymptotic confidence interval proposed in<sup>28</sup>. Together with<sup>29</sup>, these authors suggest that the asymptotic confidence interval can be a good approximation of the uncertainty in the optimal parameters  $u^*$  providing that, besides the aforementioned relation, the measurement error is relatively small as compared to the data. The formula of the confidence interval for each parameter  $u_k^*$  is given by  $CI_k := [u_k^* - \psi, u_k^* + \psi]$ , with  $\psi$  being defined as

$$\psi := \sqrt{2\chi^2(q, df) \cdot (\nabla^{-2}(-\log L(u^*)))_{kk}}. \quad (21)$$

The operator  $\nabla^{-2}$  denotes the inverse of the Hessian while  $\chi^2(q, df)$  denotes the  $q$  quantile of the  $\chi^2$  distribution with the degree of freedom  $df$ . The degree of freedom can be chosen between two that further determines the type of confidence interval:  $df = 1$  gives *pointwise asymptotic confidence interval* (PACI) that works on the individual parameter,  $df = |u|$  gives a *simultaneous asymptotic confidence interval* (SACI) that works jointly for all the parameters<sup>28</sup>.

### Numerical results

The number of iterations for Germany using the Metropolis algorithm, as well as for the preprocessing in each country should be a high number to prevent the algorithm from local minima. As of<sup>10</sup> we set this number to 20,000.

### Constant travel impact rate

For Model B with a constant value for  $\alpha$  from 15 June onwards, Tab.5 shows the mean and standard deviations for the estimated parameters of the above explained model, starting values and methods. Additionally, the pointwise asymptotic confidence interval and simultaneous asymptotic confidence interval are shown by  $\psi$  as of eq.(21).

Parameter	mean value	$\sigma$ of Metropolis	$\psi$ of PACI	$\psi$ of SACI
$\beta$	$3.06 \cdot 10^{-2} \text{d}^{-1}$	$0.03 \cdot 10^{-2} \text{d}^{-1}$	$0.03 \cdot 10^{-2} \text{d}^{-1}$	$0.20 \cdot 10^{-2} \text{d}^{-1}$
$\delta$	$6.29 \cdot 10^{-1}$	$0.09 \cdot 10^{-1}$	$0.02 \cdot 10^{-1}$	$0.42 \cdot 10^{-1}$
$\mu$	$6.74 \cdot 10^{-3}$	$0.12 \cdot 10^{-3}$	$0.01 \cdot 10^{-3}$	$0.20 \cdot 10^{-3}$
$\tau$	$2.62 \cdot 10^1 \text{d}$	$0.05 \cdot 10^1 \text{d}$	$0.0001 \cdot 10^1 \text{d}$	$0.003 \cdot 10^1 \text{d}$
$E_0$	$3.36 \cdot 10^3$	$0.06 \cdot 10^3$	$0.07 \cdot 10^3$	$1.39 \cdot 10^3$
$\alpha$	2.96	0.05	0.06	0.06

**Table 5.** Numerical Results for Model B using a constant value of  $\alpha$

Fig.2 shows the estimated disease dynamics in comparison to the registered cases using the parameters as of Tab.5.. Additionally, the uncertainty range raised by the confidence intervals of the simultaneous asymptotic confidence interval (SACI) is provided. For this, we use both the maximal and the minimal values of the SACI to show the highest and lowest possible values of the registered cumulative infected persons. The range of the pointwise asymptotic confidence interval (PACI) is comparatively low and almost no differences could be detected in the graphic. Another interesting aspect is to observe on how large the infected cases and fatalities in this model had been if  $\alpha = 0$ , i.e. the travel ban had *not* ended and travellers had no impact on the disease dynamics whatsoever; this is also included in the figure.

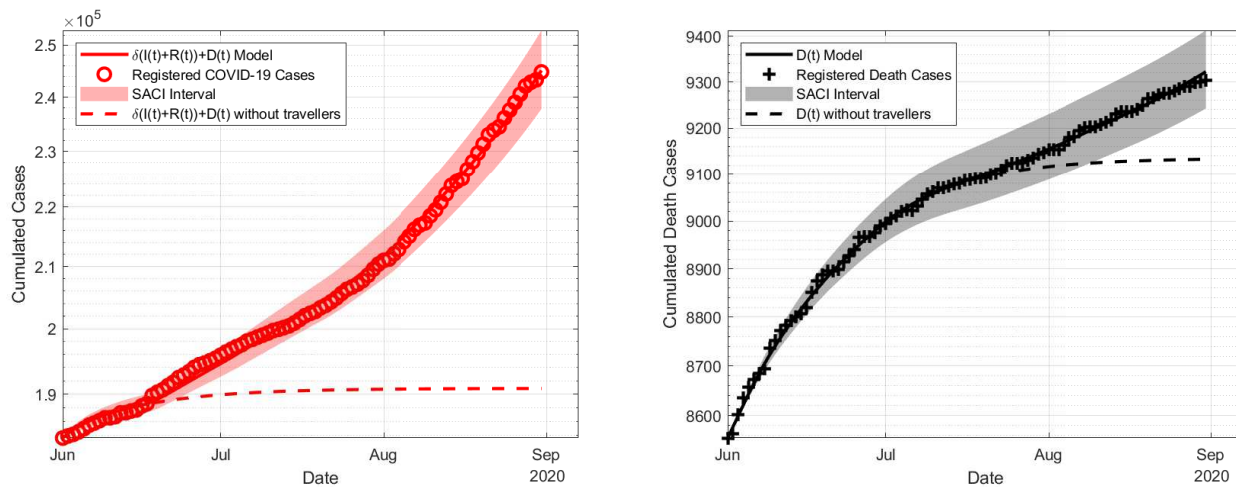


**Figure 2.** Estimation of infections in Germany compared to Johns Hopkins University from 1 June to 31 August with a constant impact rate  $\alpha$ , on the left side the cumulative number of infections, on the right side the cumulative death cases. The shaded area represents the range of the solutions from the SACI and the dashed line describes the simulation with  $\alpha = 0$ , i.e. either no travelling is allowed or the traveller compartment had been completely free of the disease.

The left graphic in Tab.5 shows that for our estimated parameter set, around 50,000 less infections with COVID-19 had been registered if the travel compartment had not been active. In the right figure concerning the death cases would make significant changes only from the end of July, resulting in a difference of roughly 150 death cases. The raised infection data obviously also has a major impact on the disease dynamics from September onwards.

### Time-dependent travel impact rate

For Model C, we now assume that  $\alpha$  is not constant over the whole time from June to August, but rather time-dependent. With  $\alpha(t)$  being piecewise constant for 15–30 June, July and August, the parameter estimation for model 3 yields the following results as to be seen in Tab.6 and Fig.3. In this figure, similar to above, we also show the range with respect to the SACI of the parameters and the scenario if no travelling had been allowed.

Parameter	mean value	$\sigma$ of Metropolis	$\psi$ of PACI	$\psi$ of SACI
$\beta$	$4.76 \cdot 10^{-2} \text{d}^{-1}$	$0.09 \cdot 10^{-2} \text{d}^{-1}$	$0.003 \cdot 10^{-2} \text{d}^{-1}$	$0.08 \cdot 10^{-2} \text{d}^{-1}$
$\delta$	$5.39 \cdot 10^{-1}$	$0.08 \cdot 10^{-1}$	$0.0003 \cdot 10^{-1}$	$0.18 \cdot 10^{-1}$
$\mu$	$5.65 \cdot 10^{-3}$	$0.19 \cdot 10^{-3}$	$0.003 \cdot 10^{-3}$	$0.09 \cdot 10^{-3}$
$\tau$	$2.67 \cdot 10^1 \text{d}$	$0.06 \cdot 10^1 \text{d}$	$0.009 \cdot 10^1 \text{d}$	$0.24 \cdot 10^1 \text{d}$
$E_0$	$2.33 \cdot 10^3$	$0.03 \cdot 10^3$	$0.002 \cdot 10^3$	$0.05 \cdot 10^3$
$\alpha_0$	2.15	0.04	0.002	0.05
$\alpha_1$	2.43	0.06	0.003	0.09
$\alpha_2$	3.29	0.04	0.005	0.12

**Table 6.** Numerical Results for piecewise constant values of  $\alpha$

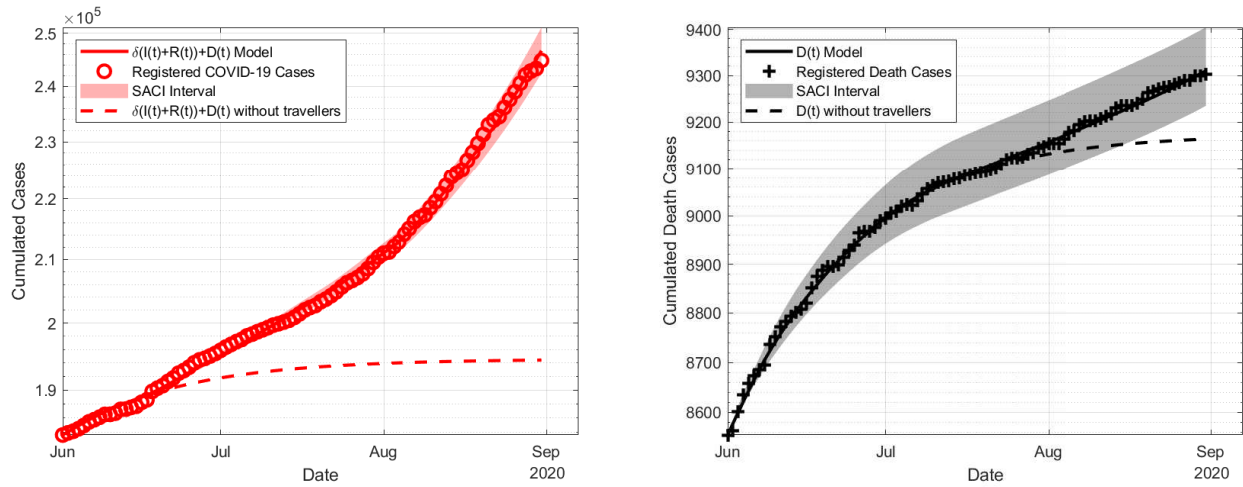


**Figure 3.** Estimation of infections in Germany compared to Johns Hopkins University from 1 June to 31 August with a piecewise constant travel impact rate  $\alpha$ , on the left side the cumulative number of infections, on the right side the cumulative death cases. The dashed line describes the simulation with  $\alpha = 0$ , i.e. either no travelling is allowed or the traveller compartment had been completely free of the disease.

### Comparison

For the Bayesian analysis, we can now compare the BIC values of the three models computed by equation (13) and (14). The results for Model A were gained by applying eqs. (3), i.e. the model we used to estimate the disease behaviour in all other countries, to Germany.

	$J(u)$	# of Parameters	BIC
Model A	$6.1304 \cdot 10^{-5}$	6	3,955.8
Model B	$2.1473 \cdot 10^{-5}$	6	3,955.1
Model C	$1.2504 \cdot 10^{-5}$	8	3,964.0

**Table 7.** Values for the least-square value  $J(u)$  and the BIC for the various models.

Tab.7 shows that in terms of the least-square output, the model with time-dependent, piecewise constant values of  $\alpha$  (Model C) shows the best results. However, due to the penalization of complexity with two more parameters, the BIC is higher, which according to<sup>20</sup> indicates a "strong" evidence that Model B using a constant value for  $\alpha$  is to be preferred.

### Sensitivity analysis

Posterior to the fitting and parameter estimation, two questions remain that we would like to focus on this section:

- (Q1) Which parameters in  $u$  need more careful specifications for which the model solutions, as well as the likelihood function, easily perturb within large orders of magnitude as the parameters slightly change?

(Q2) Which interventions should be more emphasized for different states of the parameter values that could happen in the prediction window?

These two different issues are addressed in the framework of sensitivity analysis. Its basic idea lies in the definition of a certain measure  $\mathcal{M}$  for variable change that is worth of investigation, especially when one would like to describe its sensitivity with respect to a parameter  $\vartheta$ . The sensitivity of  $\mathcal{M}$  with respect to  $\vartheta$  in the sense of first-order change can be measured with the aid of Taylor expansion. Suppose that  $\vartheta$  is increased up a certain percentage  $\varepsilon$  from its current value, i.e.,  $\vartheta \mapsto \vartheta + \varepsilon\vartheta$ . This way, the ratio  $(\vartheta + \varepsilon\vartheta)/\vartheta = 1 + \varepsilon$  returns the total percentage post perturbation and  $\varepsilon$  denotes the additional percentage of gain. Note that imposing  $\varepsilon$  as the percentage is considered more robust than as simply the increase, considering that different parameters may live in disparate scales. Now, in the similar manner as for the parameter, the total percentage in  $\mathcal{M}$  post perturbation on  $\vartheta$  is given by

$$\frac{\mathcal{M}(\vartheta + \varepsilon\vartheta)}{\mathcal{M}(\vartheta)} = 1 + \varepsilon\vartheta \frac{\partial_{\vartheta}\mathcal{M}(\vartheta)}{\mathcal{M}(\vartheta)} + \mathcal{O}(\varepsilon^2) \quad (22)$$

providing that  $\varepsilon$  is sufficiently small, i.e., first-order change. Since the percentage of gain is usually considered similar across parameters, the role of  $\varepsilon$  in the preceding equation is often neglected. The remaining expression thus provides a measurement of the sensitivity. Usually, authors refer  $\partial_{\vartheta}\mathcal{M}(\vartheta)$  as the *sensitivity index* and  $\vartheta\partial_{\vartheta}\mathcal{M}(\vartheta)/\mathcal{M}(\vartheta)$  as the *elasticity*, cf.<sup>30</sup>. Between two parameters  $\vartheta_1, \vartheta_2$ , it is logical to say that  $\mathcal{M}$  is more sensitive to  $\vartheta_1$  than  $\vartheta_2$  when the absolute normalized sensitivity indices hold the relation

$$\left| \vartheta_1 \frac{\partial_{\vartheta_1}\mathcal{M}(\vartheta_1)}{\mathcal{M}(\vartheta_1)} \right| > \left| \vartheta_2 \frac{\partial_{\vartheta_2}\mathcal{M}(\vartheta_2)}{\mathcal{M}(\vartheta_2)} \right|. \quad (23)$$

### Time-dependent measures

The question (Q1) conveys the notion of model solution and addresses what our model solutions, especially those excluded from the measurement or fitting, could have changed as we perturb the optimal parameters  $\Lambda = \{\beta, \alpha, E_T, \kappa, \mu, \gamma, \tau\}$ . Our interest is now driven by all the measures  $\mathcal{M}$  that represent model state variables  $\Psi = \{S, E, I, R, D\}$ , which apparently are time-varying. We then define the sensitivity index of state  $\psi_i \in \Psi$  with respect to parameter  $\lambda_j \in \Lambda$  as

$$S_{ij} := \frac{d}{d\lambda_j} \Psi_i. \quad (24)$$

We also included the parameters  $\gamma$  and  $\kappa$  from Table 1 although they were not optimized, yet can be assumed to bear uncertainties. As we do not obtain closed-form solutions of the state equations  $\dot{\Psi} = f(t, \Psi, \Lambda)$ , which could then be derived, an additional set of  $|\Psi|$  first-order differential equations for the sensitivity has to be deduced<sup>30</sup>:

$$S'_{ij} = \sum_k S_{kj} \cdot \frac{\partial}{\partial \psi_k} f_i + \frac{\partial}{\partial \lambda_j} f_i, \quad S_{ij}(0) = 0. \quad (25)$$

In most cases,  $\lambda_i(t) \equiv \lambda_i$  is constant, except for  $E_T$  and in one scenario  $\alpha$ , cf. next section. Fig. 4 shows the elasticities  $\lambda_j S_{ij}/\Psi_i$  around the parameter values given in tables 5 and 6, respectively. Generally  $E_T$  being the most sensitive parameter through all compartments, particularly with ongoing simulation time. Additionally, changes in the parameters  $\alpha$  and  $\gamma$  would significantly influence the infected compartment but not the death compartment, in which no parameter shows a higher elasticity than 0.15.

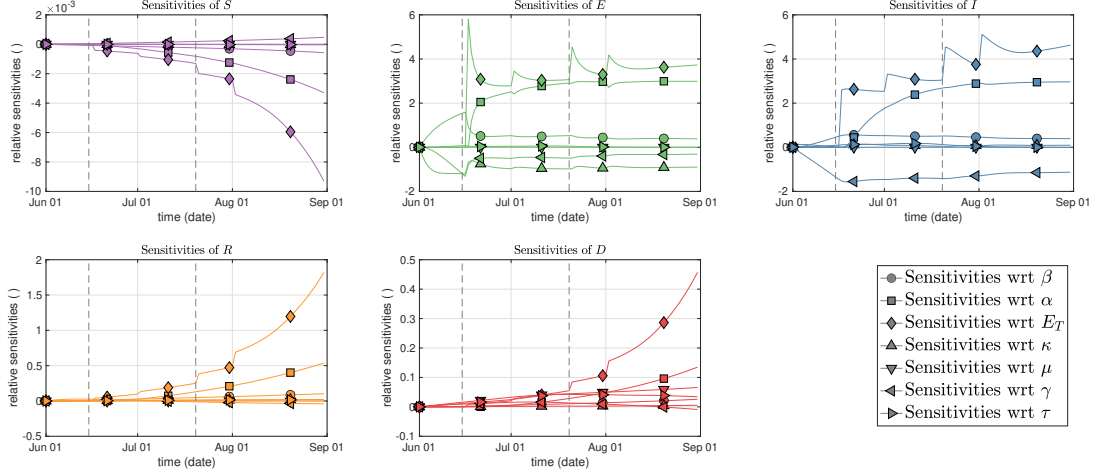


**Figure 4.** Sensitivities for the model using a time-independent travel impact rate.

After all, a caveat with these measures remains, as the elasticities are time-varying. Therefore, preference to a certain parameter for the highest elasticity could change over time.

### Time-independent measure

The question (Q2) is concerned more with interventions. In this case, we focus more on parameters that can be changed with the help of humans. In our context, such parameters could be  $\beta$  and  $\alpha$ . The direct transmission rate  $\beta$  has always been related to the proximity of the susceptible against infected humans and can be reduced with the aid of masks and social/physical distancing. The parameter  $\alpha$  is related additional factors that drive the infection more than it could have been in the origin and destination country. For example, travellers are more exposed to physical encounters with other humans during flights, in public transportation, or in touristic areas, whereas locals spend more time at home. More protective apparatuses and educational campaigns will help reduce  $\alpha$ . In this regard, two different measures for the sensitivity can be considered. For the first choice, we may take, for example,  $\mathcal{M} := \int_0^T I dt$ , which represents the total number of infected cases over all observations. If  $\alpha, \beta > 0$ ,  $\mathcal{M}$  is then more sensitive to  $\beta$  rather than  $\alpha$  when it holds

$$\beta \cdot \left| \frac{\int_0^T \partial_\beta I dt}{\int_0^T I dt} \right| > \alpha \cdot \left| \frac{\int_0^T \partial_\alpha I dt}{\int_0^T I dt} \right|. \quad (26)$$

This inequality, however, includes terms  $|\int_0^T \partial_\beta I dt|, |\int_0^T \partial_\alpha I dt|$  that do not account for entropy or state of disorder. The term  $\partial_\alpha I$  that largely fluctuates around zero can sum up to a small number and returns a small sensitivity index rather than  $\partial_\beta I$  that just delineates a “calm” trajectory above zero. To account for entropy, we shall consider the second measure

$$\mathcal{M} := \int_0^\beta \int_0^T |\partial_\beta I(t, s)| dt ds, \quad (27)$$

which represents the total variation of  $I$  with respect to  $\beta$ , evaluated up to the current parameter value. Now,  $\mathcal{M}$  is said to be more sensitive to  $\beta$  than  $\alpha$  (or vice versa) if

$$\beta \cdot \left| \frac{\int_0^T |\partial_\beta I| dt}{\int_0^\beta \int_0^T |\partial_\beta I(t, s)| dt ds} \right| > \alpha \cdot \left| \frac{\int_0^T |\partial_\alpha I| dt}{\int_0^\alpha \int_0^T |\partial_\alpha I(t, s)| dt ds} \right|. \quad (28)$$

From the computational perspective, one can define a certain grid representing domain of interest for the two parameters, for example  $[\beta_{\min}, \beta_{\max}] \times [\alpha_{\min}, \alpha_{\max}]$ . The next step follows from computing the sensitivity indices for all grid points and applies the ratio of actual total variation and accumulated total variation in (28). Therefore, the left-hand side should be done via stepping  $\alpha$  (vertical mode) and the right-hand side via stepping  $\beta$  (right mode). Finally, one may generate a two-color profile for which the inequality in (28) indeed applies or the other direction does. Fig. 5 shows the comparison of the elasticities in reasonable ranges of  $\beta$  and  $\alpha$ . For our fitted value  $(\alpha, \beta) = (2.96, 0.0306)$  we find that the measure  $\mathcal{M}$  as in (27) is more sensitive to  $\beta$  than  $\alpha$ .

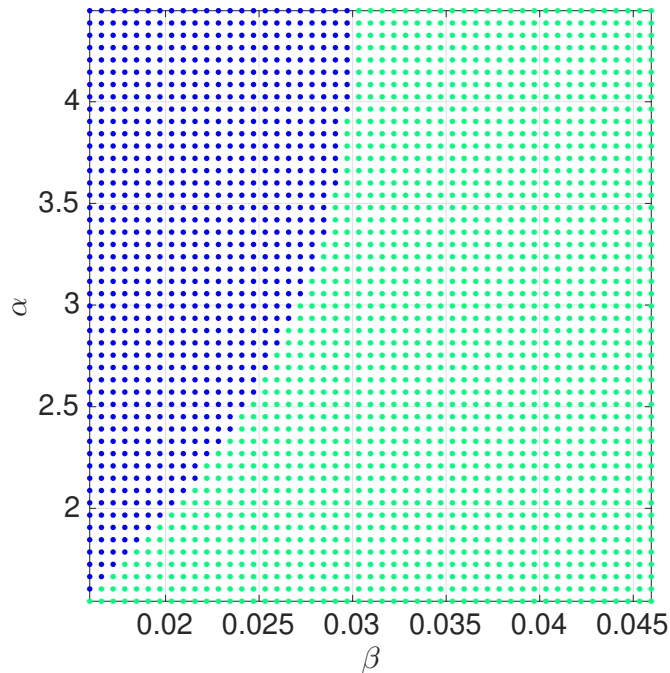


**Figure 5.** Comparison of the elasticities in a domain of interest for the transmission rate  $\beta$  and the travel impact rate  $\alpha$ . The green dots occupy the region where the elasticity of the measure  $\mathcal{M}$  as in (27) with respect to  $\beta$  is larger than that with respect to  $\alpha$ , meaning that the condition in (28) is satisfied.

This finding draws forth further practical relevance. Our model can be calibrated with new incidence data on an initial take-off period in the next winter season, where all parameters except  $\beta$  and  $\alpha$  are fixed according to our fitting. At first, the two parameters can be fitted to these new data. May they locate in one of the two regions in Fig. 5, we then acquire knowledge on which resources should be drawn in order to attack the most sensitive parameter. One can thus wait and see how the deployment of the resources gives the real-time intervention to the number of infected cases. Re-calibration then follows after some time as short-term feedback from such an intervention is gained, and the values of optimal  $\beta$  and  $\alpha$  can once again be evaluated via Fig. 5. This process of combining sensitivity-based interventions remains continuous until the ultimate disease eradication is achieved without having to waste resources.

## Conclusion

In this present work we have used several assumptions to show the impact of travellers on the overall disease dynamics in Germany during summer 2020 using a modified SEIRD-model with a traveller compartment. The sensitivities of the model with respect to the travel impact rate  $\alpha$  were calculated, showing that while the impact is not as large as the transmission rate  $\beta$ , it can be identified after a certain time delay. Travel rates are found by using international flight and hospitality data. The infection data of all 55 countries with more than 5,000 German travellers in June, July and August together has been used to optimise the single-country infections. The estimates for the transmission rates  $\beta_{j,0/1}$  in those countries are used in a multi-patch model to estimate the travel impact rate for Germany. Parameter estimation was done using a Metropolis type algorithm, while other routines like an adjoint based approach are also possible. The numerical estimations match the real data well, while they can be optimised by using a time-dependent value for the travel impact rate. In these models, the travel impact rate was estimated to be in the range of  $2 \leq \alpha \leq 3.5$ , meaning a two-to three times higher infection possibility as a traveller than the average inhabitant of the respective country. This depends on the chosen model; we compared models with constant and piecewise constant travel impact rates. While the second model lead to better values in the  $\mathcal{L}_2$  norm, the first model yields better BIC values due to less parameters being used. The raised infection rates by travellers also indirectly causes even higher cases from September onwards. Among other reasons such as seasonality and opening of schools after the summer holidays, this lead to a second large wave in late 2020<sup>2,6</sup>. This shows that travel bans are an important tool for disease control, especially when the infection cases are otherwise comparatively low. It is up to further research to regard whether a travel ban or tightening of travel restrictions had prevented this or just postponed this to a later date. Germany has experienced low infection numbers by the end of May 2021, and it is still uncertain if the high vaccination rates can prevent a potential fourth wave in autumn 2021; because of this, awareness of the dynamics of the second wave in the previous year are important. Future

work in this topic might include the impact of foreign travellers in Germany and a international network model including travellers from and to all investigated regions or countries.

## References

1. Tagesschau. Erster Coronavirus-Fall in Deutschland. <https://www.tagesschau.de/inland/coronavirus-deutschland-erster-fall-101.html> (2020). Visited on 20 November 2020.
2. Johns Hopkins University. Time series of confirmed COVID–19 cases globally. [github.com/CSSEGISandData/COVID-19/blob/master/csse\\_COVID\\_19\\_data/csse\\_COVID\\_19\\_time\\_series/time\\_series\\_COVID19\\_confirmed\\_global.csv](https://github.com/CSSEGISandData/COVID-19/blob/master/csse_COVID_19_data/csse_COVID_19_time_series/time_series_COVID19_confirmed_global.csv) (2020). Visited on 20 November 2020.
3. Anderson, R., Heesterbeek, H., Klinkenberg, D. & Hollingsworth, T. How will country-based mitigation measures influence the course of the COVID-19 epidemic? *Lancet* **395**, 931–934 (2020).
4. Federal Foreign Office of Germany. Coronavirus / Covid-19: Reisewarnung für Staaten außerhalb der EU/Schengen-Gebiet. <https://www.auswaertiges-amt.de/de/ReiseUndSicherheit/covid-19/2296762> (2020). Visited on November 20, 2020.
5. World Health Organization. Coronavirus disease (COVID-19) Weekly Epidemiological Update and Weekly Operational Update. <https://www.who.int/emergencies/diseases/novel-coronavirus-2019/situation-reports> (2019). Visited on 20 November 2020.
6. Robert–Koch–Institute. Daily situation reports. [www.rki.de/DE/Content/InfAZ/N/Neuartiges\\_Coronavirus/Situationsberichte/Gesamt.html](https://www.rki.de/DE/Content/InfAZ/N/Neuartiges_Coronavirus/Situationsberichte/Gesamt.html) (2020). Visited on 20 November 2020.
7. Berestycki, H., Roquejoffre, J.-M. & Rossil, L. Propagation of Epidemics Along Lines with Fast Diffusion. *Bull. Math. Biol.* **83**, DOI: <https://doi.org/10.1007/s11538-020-00826-8> (2020).
8. Siegenfeld, A. & Bar-Yam, Y. The impact of travel and timing in eliminating COVID-19. *Commun. Phys.* **3**, DOI: <https://doi.org/10.1038/s42005-020-00470-7> (2020).
9. Chinazzi, M. *et al.* The effect of travel restrictions on the spread of the 2019 novel coronavirus (COVID-19) outbreak. *Science* **368**, 395–400, DOI: <https://doi.org/10.1126/science.aba9757> (2020).
10. Heidrich, P., Schäfer, M., Nikouei, M. & Götz, T. The COVID–19 outbreak in Germany — Models and Parameter Estimation. *Commun. Biomath. Sci.* **3**, 37–59 (2020).
11. Kermack, W. & McKendrick, A. Contributions to the mathematical theory of epidemics–I. 1927. *Bull. Math. Biol.* **53**, 33–55 (1991).
12. Martcheva, M. *An introduction to mathematical epidemiology* (Springer, 2015).
13. United Nations, Department of Economic and Social Affairs, Population Dynamics. World Population Prospects 2019. <https://population.un.org/wpp/DataQuery/> (2019). Visited on 20 November 2020.
14. Robert–Koch–Institute. Modellierung von Beispielszenarien der SARS-CoV-2-Epidemie 2020 in Deutschland. [https://www.rki.de/DE/Content/InfAZ/N/Neuartiges\\_Coronavirus/Modellierung\\_Deutschland.pdf?\\_\\_blob=publicationFile](https://www.rki.de/DE/Content/InfAZ/N/Neuartiges_Coronavirus/Modellierung_Deutschland.pdf?__blob=publicationFile) (2020). Visited on 20 November 2020.
15. Federal Government of Germany. Vorübergehende Grenzkontrollen an den Binnengrenzen zu Österreich, der Schweiz, Frankreich, Luxemburg und Dänemark. <https://www.bmi.bund.de/SharedDocs/pressemitteilungen/DE/2020/03/grenzschliessung-corona.html> (2020). Visited on 20 November 2020.
16. Statistisches Bundesamt (Germany). Statistik über die touristische Nachfrage - Reisen: Deutschland, Jahre, Reiseverhalten, Reiseziel/Reisedauer/Reisegründe/Unterkünfte/Verkehrsmittel. [https://www.destatis.de/DE/Home/\\_inhalt.html](https://www.destatis.de/DE/Home/_inhalt.html) (2020). Visited on 20 November 2020.
17. Statistische Bibliothek. Fachserie/6/7/1/Monatlich. Wiesbaden. [https://www.statistischebibliothek.de/mir/receive/DESerie\\_mods\\_00000082](https://www.statistischebibliothek.de/mir/receive/DESerie_mods_00000082) (2020). Visited on 20 November 2020.
18. Statistische Bibliothek. Fachserie/8/6/Monatlich. Wiesbaden. [https://www.statistischebibliothek.de/mir/receive/DEHeft\\_mods\\_00132393](https://www.statistischebibliothek.de/mir/receive/DEHeft_mods_00132393) (2020). Visited on 20 November 2020.
19. Kalbfleisch, J. *Probability and Statistical Inference, Volume 1: Probability* (Springer, New York, NY, 1985).
20. Raftery, A. Bayesian Model Selection in Social Research. *Sociol. Methodol.* **25**, 111–163 (1995).
21. Akaike, H. Information Theory and an Extension of the Maximum Likelihood Principle. In Parzen, E., Tanabe, K. & Kitagawa, G. (eds.) *Selected Papers of Hirotugu Akaike* (Springer, New York, NY, 1998).

22. Götz, T. & Heidrich, P. Novel Coronavirus (2019-nCoV) situation reports (preprint). DOI: <https://doi.org/10.1101/2020.04.23.20076992> (2020).
23. Metropolis, N., Rosenbluth, A., Rosenbluth, M., Teller, A. & Teller, E. Equation of State Calculations by Fast Computing Machines. *J.Chem. Phys.* **21**, 1087–1092 (1953).
24. Gelman, A., Carlin, J., Stern, H. & Rubin, D. *Bayesian Data Analysis, 2<sup>nd</sup> Edition*. (Chapman and Hall, London, 1996).
25. Gilks, W., Richardson, S. & Spiegelhalter, D. *Markov chain Monte Carlo in Practice* (Chapman and Hall/CRC, London, 1996).
26. Schäfer, M. & Götz, T. Modelling Dengue Fever Epidemics in Jakarta. *Int. J. Appl. Comput. Math* **6** (2020).
27. Rusatsi, D. *Bayesian analysis of SEIR epidemic models*. Ph.D. thesis, Lappeenranta University of Technology (2015).
28. W.H., P., Teukolsky, S., Vetterling, W. & Flannery, B. *Numerical Recipes: The Art of Scientific Computing, 3<sup>rd</sup> edition*. (Springer, 2007).
29. Raue, A. *et al.* Structural and practical identifiability analysis of partially observed dynamical models by exploiting the profile likelihood. *Bioinformatics* **25**, 1923–1929, DOI: <https://doi.org/10.1093/bioinformatics/btp358> (2009).
30. Rockenfeller, R., Günther, M., Schmitt, S. & Götz, T. Comparative Sensitivity Analysis of Muscle Activation Dynamics. *Comput. Math. Methods Med.* DOI: <https://doi.org/10.1155/2015/585409> (2015). Article ID 585409.

## Declarations

### Ethics approval and consent to participate

Not applicable.

### Consent for publication

Not applicable.

### Availability of data

The datasets used and/or analysed during the current study which are not already cited in the article<sup>2,5,13,16–18</sup> are available from the corresponding author on reasonable request.

### Competing interests

The authors declare that there exist no competing interests.

### Funding

Not applicable.

### Authors' contributions

M.S. collected the data, conceived the model, did numerical computations, analysis and discussion. K.P.W. conceived the confidence intervals and time-independent measures for the sensitivity analysis. R.R. conceived the time-dependent measures for the confidence intervals. All authors reviewed the manuscript.

### Acknowledgements

Not applicable.

## Supplementary Files

This is a list of supplementary files associated with this preprint. Click to download.

- [CoronaandTravellingSupp.pdf](#)